



Synthesis and high-temperature thermoelectric properties of Ni₃GaSb and Ni₃InSb

Tawat Suriwong^a, Ken Kurosaki^{b,*}, Somchai Thongtem^a, Adul Harnwungmoung^b, Tohru Sugahara^b, Theerayuth Plirdpring^b, Yuji Ohishi^b, Hiroaki Muta^b, Shinsuke Yamanaka^{b,c}

^a Department of Physics and Materials Science, Faculty of Science, Chiang Mai University, Chiang Mai 50200, Thailand

^b Graduate School of Engineering, Osaka University, Suita 565-0871, Japan

^c Research Institute of Nuclear Engineering, University of Fukui, Fukui 910-8507, Japan

ARTICLE INFO

Article history:

Received 1 December 2010

Received in revised form 1 January 2011

Accepted 3 January 2011

Available online 6 January 2011

Keywords:

Ni₃GaSb

Ni₃InSb

Thermoelectric

Seebeck coefficient

Electrical resistivity

Thermal conductivity

ABSTRACT

Ni₃GaSb and Ni₃InSb were successfully synthesized by the direct reaction of Ni and GaSb or InSb. The XRD patterns and the lattice parameters of these compounds were in good agreement with the literature data. The Seebeck coefficient (*S*), the electrical resistivity (ρ), and the thermal conductivity (κ) of Ni₃GaSb and Ni₃InSb were examined in the temperature range from room temperature to 1073 K. Both compounds indicated metal-like characteristics. The power factor ($S^2\rho^{-1}$) values increased with temperature and reached maximum at 1073 K. The κ and the dimensionless figure of merit *ZT* of both samples increased with temperature. The maximum values of the *ZT* of Ni₃GaSb and Ni₃InSb were obtained at 1073 K to be 0.022 and 0.023, respectively.

© 2011 Elsevier B.V. All rights reserved.

1. Introduction

The thermoelectric (TE) technology, used for direct conversion of waste heat into electrical power is expected to substantially contribute to future power supply and sustainable energy management [1,2]. The efficiency of a material used in TE devices is determined by the dimensionless figure of merit, $ZT = S^2T/\rho\kappa$, where *S*, ρ , *T*, and κ are the Seebeck coefficient, electrical resistivity, absolute temperature, and thermal conductivity. In order to maximize *ZT* of the material, *S* is required to be the highest, but ρ and κ are the lowest. Due to their transport property interrelation, they are needed to be optimized to achieve maximum *ZT*. In recent years, several classes of bulk materials [3,4] with high *ZT* were discovered, including those found for new TE materials [5,6].

Among the III–V binary semiconductors, gallium antimonide (GaSb) and indium antimonide (InSb) have attracted considerable attention over the last several years. GaSb based binary and ternary alloys have turned out to be important candidates for applications in long wavelength lasers and photodetectors for fiber optic communications [7]. InSb has been interested in high speed applications for transistors and other devices [8,9], which is associated directly with the very low electron effective mass and high mobility [10].

Based on these interesting electrical properties, the TE properties such as *S*, ρ , and κ of GaSb and InSb have been examined [11–14]. For example, Su et al. investigated the TE properties of Zn-doped InSb single crystals and reported the maximum *ZT* value to be around 0.27 at 700 K [13]. The TE properties of In₂Te₃–InSb solid solutions were also examined [14]. Ebnalwala investigated the TE properties of GaSb bulk crystals and reported the power factor value ($8.82 \times 10^{-3} \text{ mW m}^{-1} \text{ K}^{-2}$ at 322 K) [11]. However, as for ternary compounds containing Ga, In, and Sb, the TE properties have scarcely reported.

As for *M*–(Ga or In)–Sb ternary compounds, the existing of Ni₃GaSb and Ni₃InSb have been reported by Jan and Chang [15]. These compounds exhibit the hexagonal, *P63/mmc* crystal structure – similar to that of Ni₃GaAs [16]. The melting points were determined to be >1339 K and >1364 K for Ni₃GaSb and Ni₃InSb, respectively [15]. However, the physical properties including the TE properties of these compounds are unknown at this moment. In the present study, therefore, we tried to synthesize Ni₃GaSb and Ni₃InSb and investigate the TE properties from room temperature to 1073 K.

2. Experimental

The Ni₃GaSb and Ni₃InSb ternary compounds were synthesized by direct reactions of mixtures of the stoichiometric ratios of Ni (3 N), GaSb (6 N), and InSb (5 N) in sealed silica tubes. These mixtures were processed in a series of steps: preheated at 973 K for 12 h, slowly heated up to 1323 K for 3 days, rapidly cooled to 973 K

* Corresponding author. Tel.: +81 6 6879 7905; fax: +81 6 6879 7889.
E-mail address: kurosaki@see.eng.osaka-u.ac.jp (K. Kurosaki).

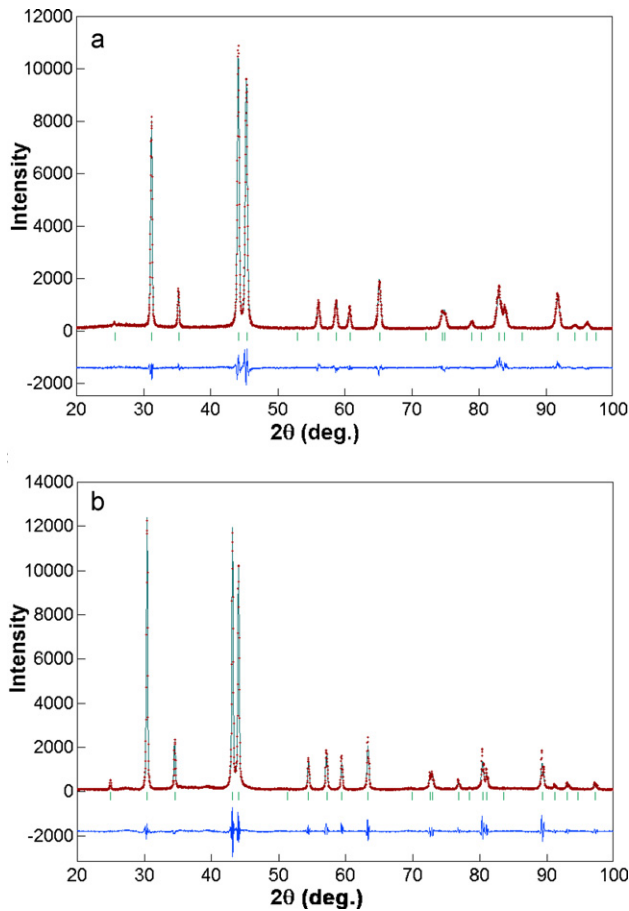


Fig. 1. Powder XRD patterns of the polycrystalline samples and the results of the Rietveld refinement of (a) Ni_3GaSb and (b) Ni_3InSb . The experimental data are shown as small red crosses, the calculated fits and the difference curves are shown as blue solid lines. Short vertical lines (green) below the patterns indicate the calculated peak positions. (For interpretation of the references to color in this figure legend, the reader is referred to the web version of this article.)

and held at this temperature for 4 days, and quenched in an ice water bath. The products were crushed and milled into fine powders. Bulk samples were then produced by spark plasma sintering (DR.SINTER LAB, SPS-515A) of the fine powders in a 20 mm diameter graphite die using 40 MPa sintering pressure at 1123 K for 30 min in an argon-flow atmosphere. The ingots were cut into the rectangular shapes of $3\text{ mm} \times 3\text{ mm} \times 15\text{ mm}$ and $10\text{ mm} \times 10\text{ mm} \times 1\text{ mm}$. Their phases, morphologies, and chemical compositions were characterized by a powder X-ray diffraction (XRD) technique using $\text{Cu K}\alpha$ radiation in a step scan condition (fixed time) with an increment of 0.02° and a slit-condition of $1.0^\circ - 1.0^\circ - 0.60\text{ mm}$ (DS-SS-RS) on Rigaku RINT 2000, and a scanning electron microscope (SEM) equipped with an energy dispersive X-ray (EDX) analyzer (Hitachi, S2600H) at room temperature. The density of the bulk samples was calculated based on the measured weight and dimensions. The electrical resistivity (ρ) and the Seebeck coefficient (S) were measured using a commercially available apparatus (ULVAC, ZEM-1) in a helium atmosphere. Thermal conductivity (κ) was evaluated from thermal diffusivity (α), heat capacity (C_p) and sample density (d) based on the relationship $\kappa = \alpha C_p d$. The thermal diffusivity was measured under vacuum by the laser flash apparatus (ULVAC, TC-7000). C_p was estimated from the Dulong–Petit model, $C_p = 3nR$, where n is the number of atom per formula unit and R is the gas constant. The TE properties were evaluated in the temperature range from room temperature to 1073 K.

3. Results and discussion

The powder XRD patterns of the prepared samples are shown in Fig. 1. Both the samples were identified as Ni_3GaSb and Ni_3InSb , according to the JCPDS database (Reference codes: 47-1401 for Ni_3GaSb and 47-1402 for Ni_3InSb) [15,17], although these compounds contained a few peaks that were inconsistent with the JCPDS data. Therefore, the XRD experimental data were analyzed by the Rietveld refinement [18] on the X-ray diffraction patterns, using

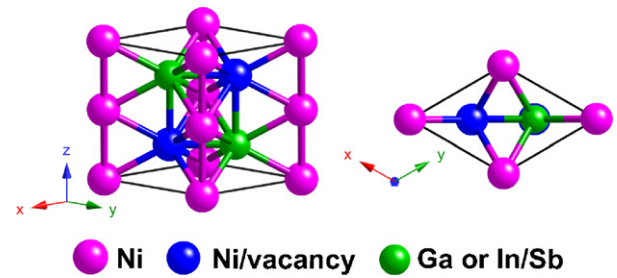


Fig. 2. Crystal structure of Ni_3GaSb and Ni_3InSb .

the hexagonal crystal system with the space group of $P63/mmc$. Details of the structure are reported in Ref. [15]. Refinement of the patterns for both compounds revealed that all the reflections can be indexed to the Ni_3GaSb and Ni_3InSb phases with no evidence of the impure phases.

The crystal structure of the compounds is described in Fig. 2. According to the crystal structure of Ni_3GaAs [16], Ni atoms occupy the $(0, 0, 0)$ and the $(0, 0, 1/2)$ positions; one vacancy and one Ni atom randomly occupy the $(2/3, 1/3, 1/4)$ and the $(1/3, 2/3, 3/4)$ positions; and Ga and As atoms randomly occupy the $(1/3, 2/3, 1/4)$ and the $(2/3, 1/3, 3/4)$ positions. The results of the Rietveld analysis for Ni_3GaSb and Ni_3InSb were in good agreement with the results of the crystal structure analysis of Ni_3GaAs .

The lattice parameters, sample bulk density, and chemical composition of the samples are summarized in Table 1. The hexagonal lattice parameters and the theoretical density of these compounds were in good agreement with those reported by Jan and Chang [15]. The densities of the polycrystalline samples taken from the sintered specimens for TE characterizations were 96% of the theoretical density. All the samples appeared to be stable in air at room temperature. The quantitative EDX analysis confirmed that the chemical compositions of the bulk sintered samples corresponded to the stoichiometric compositions, as summarized in Table 1.

The SEM and EDX mapping images of the bulk Ni_3GaSb sample are shown in Fig. 3. The SEM image indicated that the sample was homogeneous. The EDX analysis revealed that Ni, Ga, and Sb were uniformly distributed on the sample surface. As for Ni_3InSb , similar results to those for Ni_3GaSb were obtained; i.e. the SEM and EDX analyses confirmed that the Ni_3GaSb and the Ni_3InSb samples were homogeneous with stoichiometric chemical composition.

The temperature dependences of the electrical properties of the Ni_3GaSb and the Ni_3InSb samples are shown in Fig. 4. The electrical resistivity (ρ) of both samples exhibited a metal-like behavior; increased with temperature in the whole temperature range and

Table 1
Lattice parameters, sample bulk density, and chemical composition of Ni_3GaSb and Ni_3InSb .

	Ni_3GaSb	Ni_3InSb
Lattice parameter		
$a = b$ (Å)	4.0135 [4.0000]	4.1111 [4.1100]
c (Å)	5.1136 [5.0900]	5.1882 [5.1900]
Theoretical density		
d_{th} (g cm^{-3})	8.56 [8.65]	8.97 [9.03]
Measured density		
d_{exp} (g cm^{-3})	8.18	8.60
Relative density		
$d_{\text{exp}}/d_{\text{th}} \times 100$ (%)	96	96
Chemical composition determined through the EDX analysis (at.%)		
Ni	59.5	59.9
Ga	20.1	–
In	–	20.0
Sb	20.4	20.1

[], Ref. [15].

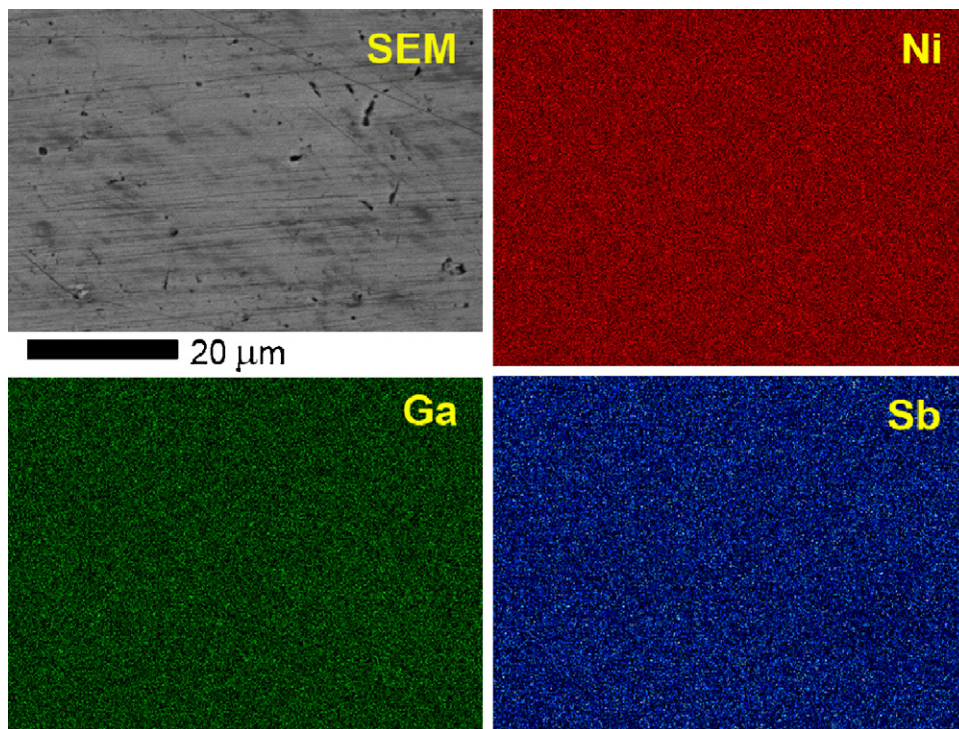


Fig. 3. SEM and EDX mapping images of the Ni_3GaSb bulk sample.

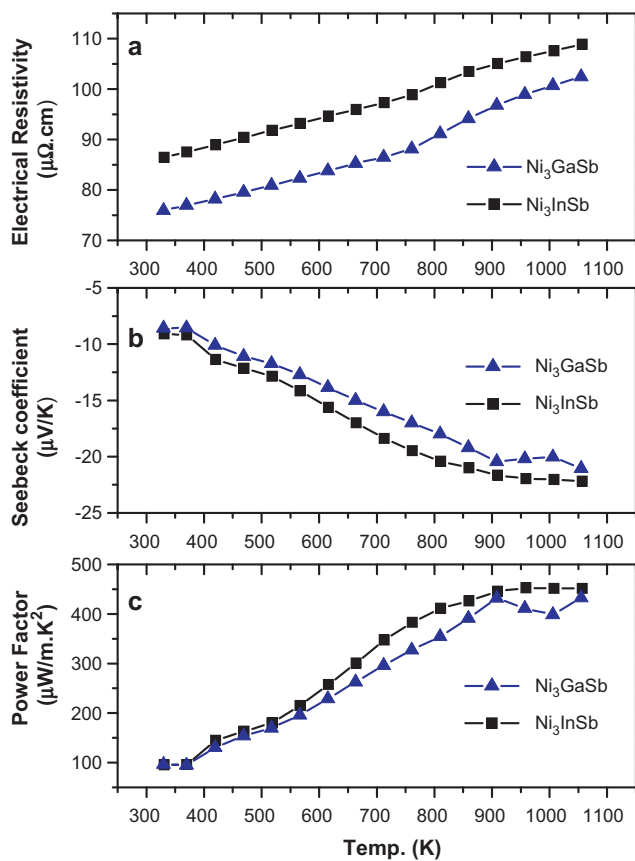


Fig. 4. Temperature dependences of the electrical properties of the polycrystalline samples Ni_3GaSb and Ni_3InSb : (a) electrical resistivity ρ , (b) Seebeck coefficient S , and (c) power factor $S^2\rho^{-1}$.

reached a maximum at 1073 K, as shown in Fig. 4(a). The Seebeck coefficient (S) values were negative for both samples, as shown in Fig. 4(b), indicating that the majority of charge carriers were electrons. The absolute S values of these samples increased with temperature and kept a constant at around 900–1073 K. The absolute S values were quite low like metals; the S values of Ni_3GaSb and Ni_3InSb at 1073 K were -21 and $-22 \mu\text{V}\text{K}^{-1}$, respectively. Ni_3GaSb exhibited the lower ρ and the lower absolute S values than those of Ni_3InSb . Since the larger carrier concentration (n) basically leads to the lower ρ and the lower absolute S , Ni_3GaSb would have the larger n values than that of Ni_3InSb . In order to discuss the magnitude relationship in the electrical properties in more detail, the Hall measurements should be performed. The power factor ($S^2\rho^{-1}$) data of the samples are plotted in Fig. 4(c), as a function of temperature. The power factor was increased with temperature and kept a constant at around 900–1073 K. The maximum values of the power factor of Ni_3GaSb and Ni_3InSb were obtained at 1073 K to be 0.43 and $0.45 \text{ mW m}^{-1} \text{ K}^{-2}$, respectively. These values were larger than those of the related compounds such as pure GaSb [11] and InSb [12] bulk samples.

The temperature dependence of the thermal conductivity (κ) of the polycrystalline samples of Ni_3GaSb and Ni_3InSb is shown in Fig. 5(a). Unfortunately, the κ values of both samples were quite high like metals and increased with temperature. Ni_3GaSb presented the higher κ values than Ni_3InSb because of the larger electronic contribution on κ of Ni_3GaSb than that of Ni_3InSb . The lattice thermal conductivity κ_{lat} was obtained by subtracting the electronic thermal conductivity κ_{el} from the total (measured) thermal conductivity κ . The value of κ_{el} was calculated using $\kappa_{\text{el}} = L\sigma T$, where σ is the electrical conductivity ($=1/\rho$) and L is the Lorentz number ($L = 2.45 \times 10^{-8} \text{ W}\Omega\text{K}^{-2}$). Room temperature values of the κ_{lat} for Ni_3GaSb and Ni_3InSb were 3.2 and $2.3 \text{ W m}^{-1} \text{ K}^{-1}$, respectively. These relatively low κ_{lat} of Ni_3GaSb and Ni_3InSb would be caused by their complex crystal structure containing a lot of vacancies as described previously. The heavier molecular weight of Ni_3InSb than that of Ni_3GaSb would lead to the lower κ_{lat} of Ni_3InSb than that of Ni_3GaSb . Note that here the calculated κ_{el}

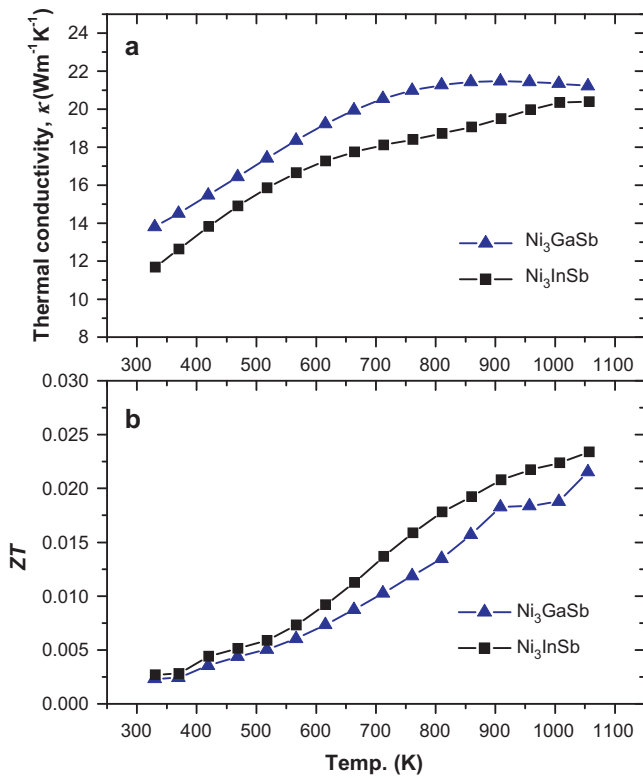


Fig. 5. Temperature dependences of the (a) thermal conductivity κ and (b) dimensionless figure of merit ZT of the polycrystalline samples of Ni_3GaSb and Ni_3InSb .

exhibited larger values than the measured κ at high temperatures, i.e. $\kappa_{\text{lat}} < 0$. This is likely due to (1) the sample for measuring ρ and κ is not the same sample, i.e. one is $3 \text{ mm} \times 3 \text{ mm} \times 15 \text{ mm}$ for ρ measurements, the other is $10 \text{ mm} \times 10 \text{ mm} \times 1 \text{ mm}$ for κ measurements; (2) at high temperature the Lorentz number ($L = 2.45 \times 10^{-8} \text{ W}\Omega \text{ K}^{-2}$) may be not valid; and (3) there exists a difference in experimental uncertainties between ρ and κ measurements. Fig. 5(b) shows the temperature dependence of the dimensionless figure of merit ZT of the samples of Ni_3GaSb and Ni_3InSb . The ZT values of both samples increased with temperature and reached maximum values at 1073 K to be 0.022 and 0.023 for Ni_3GaSb and Ni_3InSb , respectively.

4. Summary

In the present study, Ni_3GaSb and Ni_3InSb were successfully synthesized and the electrical resistivity (ρ), the Seebeck coefficient (S), and the thermal conductivity (κ) were examined from room temperature to 1073 K. The XRD patterns and the lattice parameters were in good agreement with the previously reported data. The crystal structure was hexagonal with the space group of $P63/mmc$. The ρ of both compounds increased with temperature, indicating a metal-like behavior. The S values were negative for both samples and the absolute values were low ($< 10 \mu\text{V K}^{-1}$ at room temperature for both compounds) like metals. Ni_3GaSb exhibited the lower ρ and absolute S values than those of Ni_3InSb , most likely due to the larger carrier concentration of Ni_3GaSb than that of Ni_3InSb . The κ and the ZT values of both samples were increased with temperature. The maximum values of the ZT of Ni_3GaSb and Ni_3InSb were obtained at 1073 K to be 0.022 and 0.023, respectively.

Acknowledgments

We are grateful to the Thailand Research Fund (TRF) through Royal Golden Jubilee Ph.D. Program (RGJ-Ph.D.); grant number PHD/0078/2550, Thailand for financial support, and the Graduate School of Chiang Mai University for general funding.

References

- [1] T.M. Tritt, M.A. Subramanian, *MRS Bull.* 31 (2006) 188.
- [2] D.M. Rowe (Ed.), *CRC Handbook of Thermoelectrics*, CRC Press, New York, 1995.
- [3] G.J. Snyder, E.S. Toberer, *Nat. Mater.* 7 (2008) 105.
- [4] H. Kleinke, *Chem. Mater.* 22 (2010) 604.
- [5] J.P. Heremans, V. Jovovic, E.S. Toberer, A. Saramat, K. Kurosaki, A. Charoenthaldee, S. Yamanaka, G.J. Snyder, *Science* 321 (2008) 554.
- [6] K. Kurosaki, A. Kosuga, H. Muta, M. Uno, S. Yamanaka, *Appl. Phys. Lett.* 87 (2005) 061919.
- [7] F. Capasso, M.B. Panish, S. Sumski, P.W. Foy, *Appl. Phys. Lett.* 36 (1980) 165.
- [8] R.G. van Welzenis, B.K. Ridley, *Solid State Electron.* 27 (1984) 113.
- [9] R.J. Egan, V.W.L. Chin, T.L. Tansley, *Semicond. Sci. Technol.* 9 (1994) 1591.
- [10] N.K. Udayashankar, H.L. Bhat, *Bull. Mater. Sci.* 24 (2001) 445.
- [11] A.A. Ebnalwaled, *Mater. Sci. Eng. B* 174 (2010) 285.
- [12] A.A. Ebnalwaled, *J. Cryst. Growth* 311 (2009) 4385.
- [13] X.L. Su, H. Li, X.F. Tang, *J. Phys. D: Appl. Phys.* 43 (2010) 015403.
- [14] Y. Pei, D.T. Morelli, *Appl. Phys. Lett.* 94 (2009) 122112.
- [15] C.H. Jan, Y.A. Chang, *J. Mater. Res.* 6 (1991) 2660.
- [16] T. Sands, V.G. Keramidias, J. Washburn, R. Gronsky, *Appl. Phys. Lett.* 48 (1986) 402.
- [17] Powder Diffract. File, JCPDS-ICDD, 12 Campus Boulevard, Newtown Square, PA 19073-3273, USA, 2001.
- [18] F. Izumi, K. Momma, *Solid State Phenom.* 130 (2007) 15–20.